DOI: 10.1002/chem.200700803

Intramolecular Triarylmethane–Triarylmethylium Complexes with a Naphthalene-1,8-diyl Skeleton: Isolation, Structure, and Reactivities of the C−H-Bridged Carbocations

Takashi Takeda, Hidetoshi Kawai, Kenshu Fujiwara, and Takanori Suzuki*[a]

Abstract: Isolation and low-temperature X-ray analyses of intramolecular triarylmethane–triarylmethylium complexes with a naphthalene-1,8-diyl-type skeleton have been achieved. These bridged cations prefer a C−H localized structure both in solution and in the solid state. The bridging hydrogen undergoes a facile intramolecular 1,5-hydride shift from one carbon to another in solution. The C−H delocalized geometry is suggested to be the transition-state structure of the degenerate rearrangement. Charge-transfer interaction from the triarylmethane to the triarylmethylium units is evident in the electronic spectra. This interaction stabilizes the present cations. Low reactivity toward Brønsted acids indicates that these species are not the reaction intermediates in the acid-assisted long-bond cleavage of 1,1,2,2-tetraarylacenaphthene derivatives.

Keywords: carbocations · charge transfer · hydride shift · neighboring-group effects · *peri*-interactions

Introduction

Multicentered bonds are of interest owing to their unique nature and special properties. Electron-deficient early s- and p-block elements are often involved in these intriguing bonds. Representative compounds include boranes with a three-center, two-electron (3c–2e) bond.[1] In contrast, 3c bonds of C−H−C are much less common,[2] despite the pioneering work by the groups of Sorensen and McMurry who observed the delocalized $[C-H-C]^+$ 3c–2e bond in caged hydrocarbons in strong acidic media.[3] These bridged cations show peculiar spectral features, such as very high-field resonance in ^{1}H NMR and a small coupling constant (J(C,H)) in ^{13}C NMR spectra. The delocalizability of the bridging hydrogen in the $[C\cdots H\cdots C]^+$ unit has been suggested to be sensitive to the geometry of the three-atom array,[4] which is defined by the C···H···C angle (θ), the C···C distance (D), and two kinds of C···H distances (d_1 and d_2) (Scheme 1). However, detailed studies of the geometry–delocalizability relationship have been hampered by their high reactivity, which prevents their isolation for X-ray structural analyses. Although high-level calculations have suggested that the carbon-based multicentered bonds have interesting features,[4b] the theoretical predictions still need to be verified experimentally.

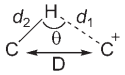

Scheme 1. Geometrical parameters for $[C\cdots H\cdots C]^+$-bridged cations.

We envisaged that incorporation of a stable carbocationic moiety into the $[C\cdots H\cdots C]^+$ unit would provide the chance to isolate the species for the first time. Therefore, triarylmethyliums, such as Ph_3C^+ or 9-phenylacridinium,[5] were selected for this purpose, and the symmetric (pseudo-symmetric) triarylmethane–triarylmethylium complexes $[Ar_3C\cdots H\cdots CAr_3]^+$ were formulated to explore the detailed structure and reactivities of the novel $[C\cdots H\cdots C]^+$-bridged carbocations. The naphthalene-1,8-diyl skeleton has attracted considerable attention owing to the significant *peri*-interaction between the two subunits at the 1,8-positions.[6] To facilitate $[C\cdots H\cdots C]^+$ bridging despite the sterically hindered triarylmethane-type structure, a series of cations (**1**) with this arylene spacer were designed and synthesized in this study. In acridan–acridinium complexes **1a–c**$^+$, the $[C\cdots H\cdots C]^+$ bridging geometry can be finely tuned by replacing the acenaphthene-5,6-diyl and acenaphthylene-5,6-diyl skeletons by naphthalene-1,8-diyl, which provides information on the relationship between the properties and the

[a] T. Takeda, Dr. H. Kawai, Prof. K. Fujiwara, Prof. T. Suzuki
Department of Chemistry, Faculty of Science, Hokkaido University
Kita 10, Nishi 8, Kita-ku, Sapporo, 060-0810 (Japan)
Fax: (+81) 11-706-2714
E-mail: tak@sci.hokudai.ac.jp

Supporting information for this article is available on the WWW under http://www.chemeurj.org/ or from the author.

 © 2007 Wiley-VCH Verlag GmbH & Co. KGaA, Weinheim

bridging distances (D, d_1, and d_2). The thermodynamic stability (pK_R^+) of the cationic moiety might also perturb the delocalizability of the bridging hydrogen. Thus, dianisylmethylium (**1d**$^+$) or diphenylmethylium (**1e**$^+$) is substituted for the acridinium unit in **1a**$^+$.[7] In this report, we describe the isolation and detailed geometrical investigation of **1a**-**e**$^+$.[8]

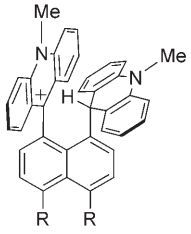

1a$^+$: R=H
1b$^+$: R-R=CH_2-CH_2
1c$^+$: R-R=CH=CH

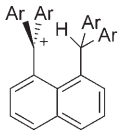

1d$^+$: Ar=An
1e$^+$: Ar=Ph

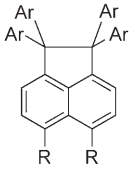

2a: Ar_2C=10-methyl-9-acridan; R=H
2b: Ar_2C=10-methyl-9-acridan; R-R=CH_2-CH_2
2c: Ar_2C=10-methyl-9-acridan; R-R=CH=CH
2d: Ar=An; R=H
2e: Ar=Ph; R=H

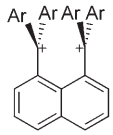

3a^{2+}: Ar_2C^+=10-methyl-9-acridinium; R=H
3b^{2+}: Ar_2C^+=10-methyl-9-acridinium; R-R=CH_2-CH_2
3c^{2+}: Ar_2C^+=10-methyl-9-acridinium; R-R=CH=CH
3d^{2+}: Ar=An; R=H
3e^{2+}: Ar=Ph; R=H

After starting this work,[9] important papers on the bridged cations $[Si\cdots H\cdots Si]^+$ and $[P\cdots H\cdots P]^+$ with the same naphthalene-1,8-diyl arylene spacer were published,[10] which allows comparisons with our purely organic counterpart. It would be particularly interesting to determine whether the bridging hydrogen in cations **1** prefers the localized position (form **A** in Scheme 2) or the delocalized position (form **B**) to better understand the nature of $[C{-}H{-}C]^+$ 3c–2e bonding.[11]

Results and Discussion

Generation and isolation of [C···H···C]$^+$-bridged cations: A bridged cation with a $[C\cdots H\cdots C]^+$ unit was recently postulated by Gabbaï and Wang as a short-lived intermediate for the acid-promoted long-bond fission of 1,1,2,2-tetraanisylacenaphthene (**2d**) to form the corresponding dication **3d**$^{2+}$.[12] While direct protonation[3b,13] of the long C–C bond[14] with a raised sigma-orbital level is an attractive idea, we have obtained experimental results[15] that suggest that molecular oxygen is involved in this type of bond cleavage.[16] Because the direct conversion of acenaphthene **2** by protonation or the partial hydride addition of dications **3**$^{2+}$ seems to be unreliable for the isolation of novel cations **1**$^+$ in pure form, we planned the synthetic routes shown in Schemes 3 and 4, in which the neutral precursors are converted in the final stage into the desired cations by quaternization (**1a–c**$^+$) or under dehydrating conditions (**1d**$^+$ and **1e**$^+$). In the former case, **1a–c**$^+$ could be generated under nonacidic conditions, and thus the bridged cations would remain intact in the reaction mixtures even if they were sensitive to acidic conditions, as proposed.[12]

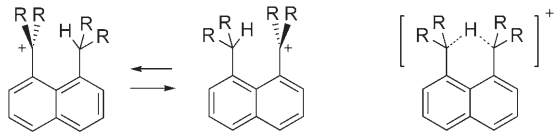

form **A** form **B**

Scheme 2. Two possible structures for $[C\cdots H\cdots C]^+$-bridged cations.

We started our preparation of acridan–acridinium complex **1a**$^+$ from 1,8-dibromoacenaphthene.[17] Under modified conditions,[18] the Stille reaction with 9-trimethylstannylacridine gave diacridine **4a**, which was selectively mono-*N*-methylated with MeOTf. Hydride addition by using $NaBH_4$ gave precursor **5a**. Final quaternization with MeOTf proceeded smoothly, and the desired cation **1a**$^+$ was obtained as a stable dark-green OTf^- salt. Similar reactions starting with *peri*-fused dibromides[19,20] gave **1b**[OTf] and **1c**[OTf]. Cations with the deuterium bridge, [D_1]**1a–c**$^+$, were obtained by using $NaBD_4$ instead of $NaBH_4$ in the reduction step.

Encouraged by the successful isolation of **1a–c**$^+$, bridged cations **1d**$^+$ and **1e**$^+$ with a cationic unit that has a smaller pK_R^+ value were prepared from 8-diarylmethylnaphthoic acids **6d** and **6e**.[21,22] Methyl ester **7d** was treated with anisyllithium to give carbinol **8d**. Under dehydrating conditions, acid treatment gave **1d**[BF_4] as a surprisingly stable dark-red solid. Though less stable than **1d**$^+$, cationic hydrocarbon **1e**$^+$ was also generated from **8e**[23] and isolated as a moisture-sensitive dark-green BF_4^- salt. Cations **1d**$^+$ and **1e**$^+$ were stable under acidic conditions, which is in contrast to the assumption[12] that **1d**$^+$ would have been transformed into dication **3d**$^{2+}$ upon contact with acid.

Preferred geometry in solution—variable temperature NMR (VT-NMR) analyses and deuterium labeling: The ^1H NMR spectra of acridan–acridinium complexes **1a–c**[OTf] in CD_2Cl_2 are C_{2v}-symmetric at room temperature with only one *N*-methyl resonance at $\delta = 3.91$, 3.94, and 3.99 ppm, re-

 © 2007 Wiley-VCH Verlag GmbH & Co. KGaA, Weinheim

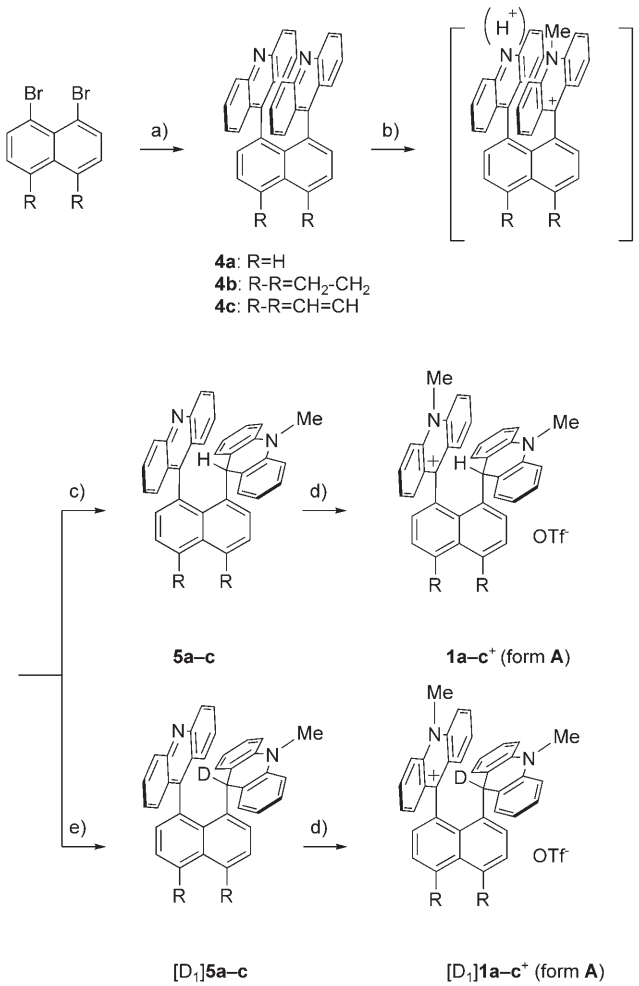

Scheme 3. Preparation of acridan–acridinium complexes **1a–c**$^+$: a) 9-trimethylstannylacridine, $[Pd(PPh_3)_4]$, CuO, *N*,*N*-dimethylformamide, 140 °C; b) MeOTf, CH_2Cl_2 (for **4a** and **4b**) or MeOTf, 2,6-di-*tert*-butyl-4-methylpyridine (for **4c**), PhH 23 °C; c) $NaBH_4$, EtOH, 23 °C; d) MeOTf, 2,6-di-*tert*-butyl-4-methylpyridine, PhH, 23 °C; e) $NaBD_4$, EtOH, 23 °C. Tf = trifluoromethanesulfonyl.

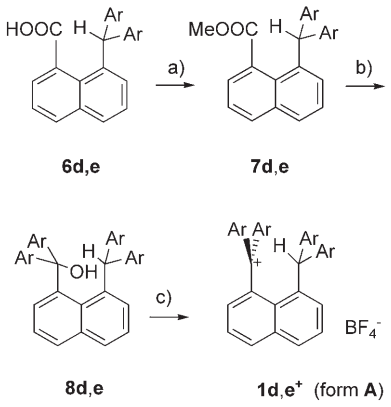

Scheme 4. Preparation of Ar_2CH-Ar_2C^+ complexes **1d**$^+$ and **1e**$^+$: a) CH_2N_2, diethyl ether/THF 23 °C; b) AnLi, diethyl ether, −78 °C (for **7d**) or PhLi, THF, −78 °C (for **7e**); c) Aqueous HBF_4, trifluoroacetic anhydride, CH_2Cl_2, 23 °C. THF = tetrahydrofuran. An = 4-methoxyphenyl.

spectively. This observation can be rationalized by assuming either a rapid degenerated 1,5-hydride shift (form **A**) or delocalized 3c–2e bond formation (form **B**). With a decrease in temperature, most of the resonances became broad. Sharp C_s-symmetric spectra were obtained for **1b**$^+$ and **1c**$^+$ at −90 °C with two distinct *N*-methyl resonances at $\delta = 4.81$ (acridinium) and 3.13 ppm (acridan) for **1b**$^+$, and 4.86 and 3.16 ppm for **1c**$^+$, respectively (Figure 1), although that of

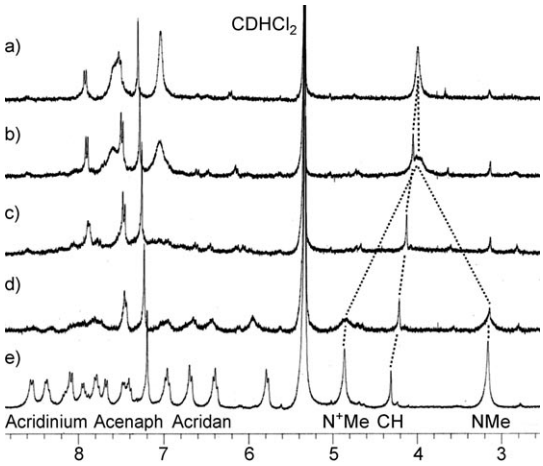

Figure 1. VT-NMR spectra of **1c**[OTf] in CD_2Cl_2 at a) 10, b) −20, c) −45, d) −65, and e) −85 °C.

1a$^+$ is just on the edge of coalescence at this temperature. The observed temperature-dependent spectral changes suggest that the bridging hydrogen is localized on one of the C9 carbons in solution and fluctuates between two equivalent sites. The chemical shift of this hydrogen (0 °C) is $\delta = 4.00$ and 3.90 ppm for **1a**$^+$ and **1b**$^+$, respectively; that of **1c**$^+$ was not clearly seen owing to peak overlap. These values are close to those of precursor **5a–c** ($\delta = 4.52$, 4.36, and 4.43 ppm, respectively), but are far different from the very high-field values that are characteristic of delocalized 3c–2e bonding hydrogens.[3f,4a,24]

The ^{13}C NMR spectra of **1b**$^+$ and **1c**$^+$ at −90 °C are also consistent with C_s-symmetric form **A** and exhibit two distinct resonances for C9: $\delta = 163.63$ and 42.33 ppm for **1b**$^+$, and 161.6 and 37.9 ppm for **1c**$^+$, respectively. The ^{13}C–^1H coupling constants (126 Hz for **1b**$^+$ and 128 Hz for **1c**$^+$, respectively) are comparable to those of corresponding precursors **5b** and **5c** (128 Hz for **5b**, 129 Hz for **5c**, respectively), which indicates the full bonding character between the bridging hydrogen and one of the C9 carbons. We measured the ^2H NMR spectrum of [D_1]**1a–c**$^+$ with a bridging deuterium atom in order to perform the $\Delta\delta$ test (^1H, ^2H) of Altman and Forsen.[25] The very small values ($-0.01 \approx -0.02$ ppm at −60 °C) indicate a deep double-minimum potential for the bridging hydrogen. These results clearly show that acridan–acridinium complexes **1a–c**$^+$ prefer a C–H localized geometry (form **A**) in solution.

The facile 1,5-hydride shift is the most characteristic process in these cations, and the energy barriers ($\Delta G^{\neq}$) were

 © 2007 Wiley-VCH Verlag GmbH & Co. KGaA, Weinheim

determined by VT-NMR analyses. The value for $\mathbf{1b}^+$ in CD_2Cl_2 is 9.6 kcal mol^{-1} ($T_c = -55$ °C for *N*-methyl protons at 300 MHz). In more polar and Lewis basic [D_6]acetone, a larger value of 10.1 kcal mol^{-1} was obtained ($T_c = -43$ °C), which suggests that the transition state is less polar than that for $\mathbf{1b}^+$ owing to charge delocalization over the two acridine-based subunits. When deuterium is substituted for the bridging hydrogen, the barrier increases as expected. The values for [D_1]$\mathbf{1b}^+$ (10.4 kcal mol^{-1} in CD_2Cl_2; 10.7 kcal mol^{-1} in [D_6]acetone) correspond to the marginal primary isotope effect ($k_H/k_D \approx 2.5$). Thus, tunneling effects are not important for the hydride shift in $\mathbf{1b}^+$.

The activation barriers of the hydride shift in $\mathbf{1c}^+$ show a similar trend in terms of solvent effects ($\mathbf{1c}^+ = 10.1$ kcal mol^{-1} in CD_2Cl_2; 10.9 kcal mol^{-1} in [D_6]acetone) as well as isotope effects ([D_1]$\mathbf{1c}^+ = 10.6$ kcal mol^{-1} in CD_2Cl_2; 11.7 kcal mol^{-1} in [D_6]acetone). All of the values are slightly larger than the corresponding values for $\mathbf{1b}^+$ and [D_1]$\mathbf{1b}^+$, which shows that the change of the *peri*-bridge from ethano to etheno induces perturbation of the [C···H···C]$^+$ geometry. As confirmed by comparisons of X-ray structures (see below), the C···C distance (D) is slightly wider in $\mathbf{1c}^+$ [3.031(4) Å] than in $\mathbf{1b}^+$ [3.004(4) Å], which is responsible for the increase in $\Delta G^{\neq}$ for the 1,5-shift. In the case of $\mathbf{1a}^+$ [$D = 2.951(9)$ Å], the separation of two acridine-based subunits at the 1,8-positions of naphthalene is noticeably narrower owing to the lack of a bridge on the opposite *peri*-position,[26] so that the 1,5-shift should be much faster than in $\mathbf{1b}^+$ and $\mathbf{1c}^+$.

The ^{1}H NMR spectrum of naphthalene derivative **1a**[OTf] shows essentially the same features and temperature-dependence as those of $\mathbf{1b}^+$ and $\mathbf{1c}^+$, but the much lower T_c corresponds to a smaller $\Delta G^{\neq}$ value (8.4 kcal mol^{-1} for [D_1]$\mathbf{1a}^+$ in [D_6]acetone, $T_c = -80$ °C). For $\mathbf{1a}^+$ or even for [D_1]$\mathbf{1a}^+$ in CD_2Cl_2, T_c is very close to or even lower than the freezing point of the solvent, suggesting that $\Delta G^{\neq}$ is less than 8 kcal mol^{-1} in these cases. The smaller energy barrier for the hydride shift corresponds to the greater flexibility of the naphthalene skeleton, which allows two acridine-based subunits to come closer to achieve a low-energy transition-state geometry with a narrower C···C separation. Based on the observed solvent effects for the series of $\mathbf{1a}$–$\mathbf{c}^+$ and [D_1]$\mathbf{1a}$–$\mathbf{c}^+$, it is highly probable that the transition state for the degenerated 1,5-hydride shift of $\mathbf{1}^+$ (form **A**) adopts a geometry close to that of the charge-delocalized form **B**.

Not only acridan–acridinium complexes $\mathbf{1a}$–$\mathbf{c}^+$, but also $\mathbf{1d}^+$ and $\mathbf{1e}^+$, show temperature-dependent NMR spectra: C_{2v}-symmetric above T_c and C_s-symmetric below T_c. The *O*-methyl groups of $\mathbf{1d}^+$ resonate at $\delta = 3.99$ (dianisylmethylium) and 3.90 ppm (dianisylmethyl) below T_c of −55 °C (300 MHz), which correspond to a $\Delta G^{\neq}$ value of 9.8 kcal mol^{-1} in CD_2Cl_2. In [D_6]acetone, $\Delta G^{\neq}$ was determined to be 10.4 kcal mol^{-1}. For $\mathbf{1e}^+$ with phenyl substituents, $\Delta G^{\neq}$ was estimated from the coalescence of naphthalene protons (9.6 kcal mol^{-1} in CD_2Cl_2). The bridging hydrogen appeared at $\delta = 5.47$ and 5.30 ppm for $\mathbf{1d}^+$ and $\mathbf{1e}^+$, respectively, which are shifted slightly downfield compared with those for $\mathbf{1a}$–$\mathbf{c}^+$. This indicates, regardless of pK_R^+ for the cationic moiety, that triarylmethane–triarylmethylium complexes $\mathbf{1}^+$ prefer a C–H localized geometry of form **A**. The bridging hydrogen undergoes a rapid 1,5-shift, whose energy barrier depends on the [C···H···C]$^+$ geometry. Compared with the acridine-based cation $\mathbf{1a}^+$, cations $\mathbf{1d}^+$ and $\mathbf{1e}^+$ with Ar_2C units exhibit a larger $\Delta G^{\neq}$ value, which can be accounted for by considering the wider separation of C···C in $\mathbf{1d,e}^+$ than in $\mathbf{1a}^+$ (see below).

Preferred geometry in the solid state (X-ray analyses) and as isolated species (theoretical calculation): The detailed geometrical parameters of the present cations were successfully obtained by X-ray analyses of all of the salts of $\mathbf{1a}$–$\mathbf{e}^+$. They are the first series of experimentally determined structures for the degenerately-rearranged/delocalized [C···H···C]$^+$-bridged cations.[11] By conducting the measurements at low temperatures, the parameters were determined with sufficient accuracy, and the bridging hydrogen atoms were located on the D maps. No positional disorders were observed around the [C···H···C]$^+$ bridge.

Regardless of their different packing arrangements, one of the acridine units in $\mathbf{1a}$–$\mathbf{c}^+$ has a planar acridinium with an sp^2-hybridized C9 carbon (sum of C-C-C bond angles = 359.8–360.1°), whereas the other is a butterfly-shaped acridan unit with an sp^3-hybridized C9 (342.0–343.5°, Table 1, Figure 2, Figures S6–S8). The latter values are close to that found for the acridan unit of precursor **5a** (343.0°) deter-

Table 1. List of geometrical parameters in $\mathbf{1a}$–$\mathbf{e}^+$ determined by X-ray analyses of their OTf^- or BF_4^- salts and those estimated by calculations (B3LYP/6-31G*).

		D	d_1	d_2	θ	ΣC-C$^+$-C	ΣC-CH-C
$\mathbf{1a}^+$	X-ray	2.951(9)	2.12(5)	0.97(6)	158(4)	359.8	342.9
	calcd	2.999	2.047	1.102	142.7	359.3	339.1
$\mathbf{1b}^+$	X-ray	3.004(4)	2.13(3)	1.03(3)	140(2)	360.0	343.5
	calcd	3.008	2.148	1.102	141.6	359.7	339.1
$\mathbf{1c}^+$	X-ray	3.031(4)	2.19(3)	0.99(4)	141(3)	360.1	342.0
	calcd	3.110	2.170	1.102	141.6	359.6	338.8
$\mathbf{1d_1}^+$	X-ray	3.082(10)	2.39(4)	0.91(5)	133(4)	359.8	339.7
$\mathbf{1d_2}^+$	X-ray	3.041(10)	2.15(7)	1.22(7)	127(5)	359.6	337.4
	calcd	3.180	2.539	1.090	116.6	359.6	337.7
$\mathbf{1e}^+$	X-ray	3.051(3)	2.35(2)	0.95(2)	130(2)	359.6	337.5
	calcd	3.200	2.585	1.090	114.8	359.8	338.0

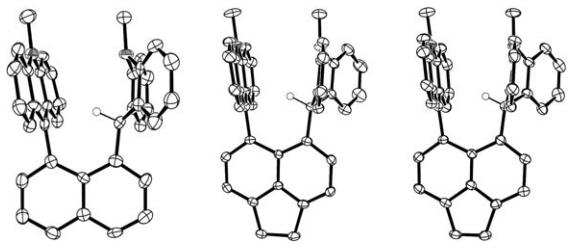

Figure 2. ORTEP drawings of bridged cations $\mathbf{1a}^+$ (left), $\mathbf{1b}^+$ (middle), and $\mathbf{1c}^+$ (right) in OTf^- salts. The counteranion, crystallization solvent (if any), and hydrogen atoms, except for the bridging one, are omitted for clarity.

© 2007 Wiley-VCH Verlag GmbH & Co. KGaA, Weinheim

mined by X-ray analysis. In the case of **1d**[BF_4] and **1e**-[BF_4], the two Ar_2C units again have different shapes: one is methylium with Csp^2 (sum of C-C-C bond angles = 359.6–359.8°) and the other is methyl with a Csp^3 carbon (337.4–339.7°, Figure 3, Figures S9–S10). In the crystal, there are no signs of a 1,5-shift of the bridging hydrogen.

The geometrical data for $[C\cdots H\cdots C]^+$ distances clearly show that the bridging hydrogen is localized on one of the C9 carbons as in form **A**. The ratios of the C···H distances (d_1/d_2) are in the range of 1.8–2.6, which is similar to the 3c–4e-type bridged cation (1.8) with a C–H localized geometry.[2] Thus, not only in solution, but also in the crystal, the preferred geometry of the bridged cations $\mathbf{1}^+$ is the C–H localized structure (form **A**).

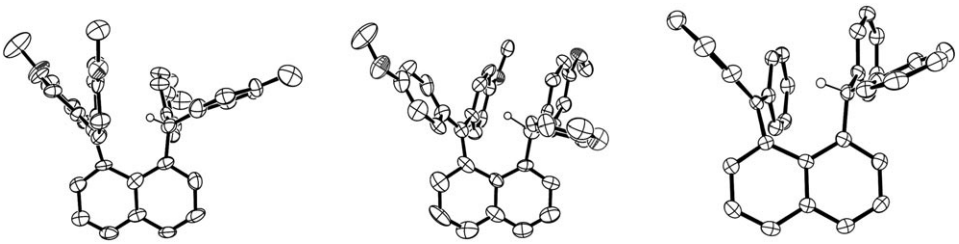

Figure 3. ORTEP drawings of bridged cations $\mathbf{1d_1}^+$ (left), $\mathbf{1d_2}^+$ (middle), and $\mathbf{1e}^+$ (right) in BF_4^- salts. The counteranion, crystallization solvent (if any), and hydrogen atoms, except for the bridging one, are omitted for clarity.

Further inspection of the geometrical data in Table 1 shows that the C···C separation (D) correlates with the energy barrier of the hydride shift ($\Delta G^{\neq}$) in solution. Thus, among the acridine-based cations **1a**–$\mathbf{c}^+$, larger values of D and $\Delta G^{\neq}$ are found for the acenaphthene and acenaphthylene derivatives $\mathbf{1b}^+$ and $\mathbf{1c}^+$ with the bridge at the opposite *peri*-position. The effects are more evident in $\mathbf{1c}^+$, which has a shorter etheno bridge. Among the naphthalene-1,8-diyl derivatives, the 1,5-hydride shift is much more facile in $\mathbf{1a}^+$ than in $\mathbf{1d}^+$ and $\mathbf{1e}^+$ because $\mathbf{1d}^+$ and $\mathbf{1e}^+$ have larger D values owing to the propeller-shaped Ar_2C^+ units.

Theoretical calculations for **1a**–$\mathbf{e}^+$ (B3LYP/6-31G*) nicely reproduced the observed solid-state structures with two differently shaped diarylmethane units (Table 1). We found no energy-minimized structure for the C–H delocalized form **B**. Thus, the preference for form **A** is not the result of crystal-packing forces or solvation effects, but rather more as a result of the intrinsic nature of cations $\mathbf{1}^+$. In accordance with such an unsymmetric geometry, the coefficients in the LUMO are mainly localized on the acridinium–diarylmethylium unit, whereas those in the HOMO are localized on the acridanyl–diarylmethyl unit (Figure 4, Figures S1–S5). A considerable portion of the coefficient is located on the bridging hydrogen. Furthermore, the unsymmetric geometry of bridged cations enables a π-type charge-transfer (CT) interaction from the diarylmethyl to the diarylmethylium units, as described in the next section. In-phase interaction of the C–H group with the cationic moiety suggests that CT also acts through the contact of $[C\cdots H\cdots C]^+$.

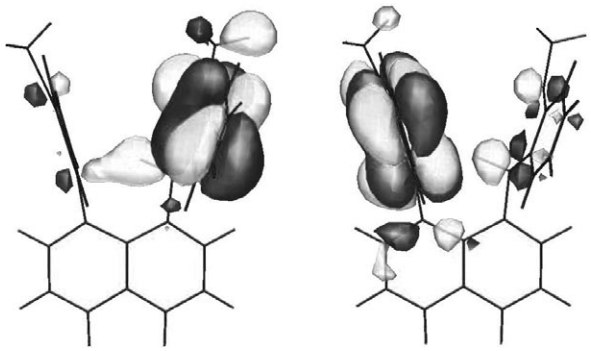

Figure 4. HOMO (left) and LUMO (right) of $\mathbf{1a}^+$ calculated at the B3LYP/6-31G* level.

Redox and spectral properties: Voltammetric analyses of acridan–acridinium complexes **1a**–$\mathbf{c}^+$ show that they exhibit moderate electrochemical amphotericity ($E_{sum} = E_{ox} - E_{red} \approx 1.4$ V, Table 2). The close proximity of the donor–acceptor units at the *peri* positions induces intramolecular CT interaction between them. Weak but significant absorptions in the long-wavelength region up to 750 nm ($\log\varepsilon \approx 3$, Figure 5, Figure S11) are assigned to the CT absorption bands of **1a**–$\mathbf{c}^+$, and the optically determined HOMO–LUMO gaps

Table 2. Redox potentials of **1a**–$\mathbf{c}^+$ measured in MeCN[a].

Compound	E_{red} [V]	E_{ox} [V]
$\mathbf{1a}^+$	−0.49	+0.90
$\mathbf{1b}^+$	−0.55	+0.81
$\mathbf{1c}^+$	−0.48	+0.85

[a] E/V versus SCE, 0.1 M Et_4NClO_4, Pt electrode, scan rate 100 mV s^{-1}.

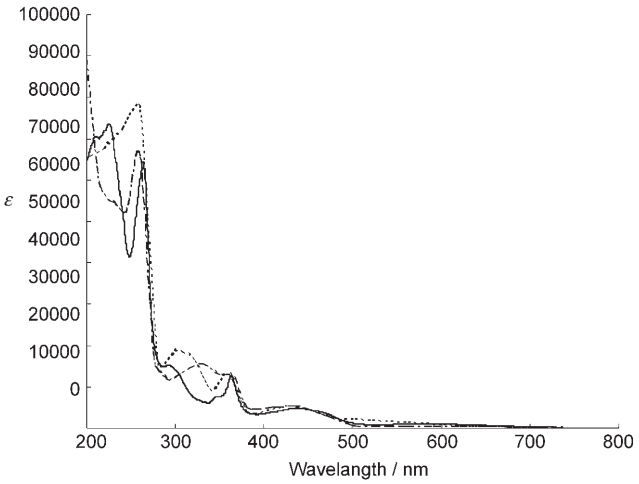

Figure 5. UV/Vis spectra of **1a** (——), **1b** (-----), and **1c** (–•–•) in MeCN.

 © 2007 Wiley-VCH Verlag GmbH & Co. KGaA, Weinheim

(1.65 eV in MeCN) correspond well to those obtained by electrochemistry (≈1.4 V in MeCN) and by calculation (1.44 eV for **1a**$^+$, 1.36 eV for **1b**$^+$, and 1.33 eV for **1c**$^+$, respectively).

One-electron reduction of bridged cations **1a–c**$^+$ is a reversible process in which the electron-deficient acridinium unit accepts the extra electron (Scheme 5). The resulting

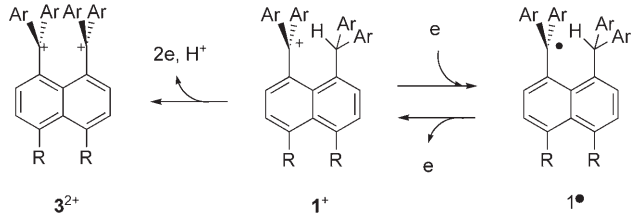

Scheme 5. Electrochemical processes of bridged cations **1**$^+$.

radicals **1a–c**$^{\bullet}$ are stable under the voltammetric conditions employed. In contrast, irreversible oxidation of the acridan unit induces C–H fission, as in the case of many triarylmethane derivatives. In fact, the return peaks were observed after irreversible oxidation of **1a–c**$^+$, whose potentials correspond to those of the reduction waves of dications **3a–c**$^{2+}$.[15] Slightly higher values of E_{ox} (+0.81–0.90 V) compared to those of the corresponding arylacridans without an acridinium unit (≈+0.78 V (irreversible) for **5a–c**) might be related to CT interaction through the hydrogen bridge.

In the case of cation **1d**$^+$ with four anisyl groups, an intramolecular CT band is not so evident in MeCN owing to the very strong local absorption of a dianisylmethylium chromophore (λ_{max} = 500 nm, log ε 5.47 for An_2C^+Ph).[7] The absorption tail at ≈700 nm is attributed to CT from An_2CH to the An_2C^+ units. The observed shoulder at ≈590 nm in CH_2Cl_2 might be attributed to CT in **1d**$^+$ (Figure 6, Figure S12).The CT band is clearly seen for **1e**$^+$ (λ_{max} = 594 nm in MeCN) owing to the higher-energy absorption for a Ph_2C^+ unit (Figure S13), which is red-shifted to 609 nm in CH_2Cl_2. Such solvent effects indicate that the ground state of **1**$^+$ is more polar than the excited state. The orbital coefficients in the HOMO of **1e**$^+$ without electron-donating heteroatoms

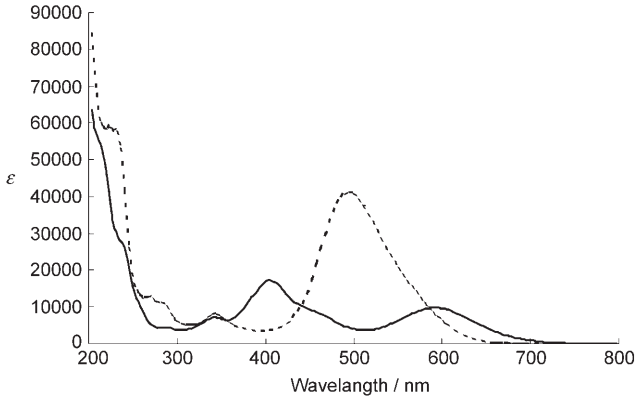

Figure 6. UV/Vis spectra of **1d**$^+$ (-----) and **1e**$^+$ (——) in MeCN.

largely depend on the torsion angle between the naphthalene core and the Ph_2C^+ unit, and the naphthalene unit may act as a stronger donating chromophore than Ph_2CH when **1e**$^+$ adopts the metastable twisted geometry. The longer-wavelength absorption in **1e**$^+$ than in **1d**$^+$ can be explained by assuming the coexistence of the metastable form in solution.

Reactivity: A dianisylmethane–dianisylmethylium bridging species with a naphthalene-1,8-diyl skeleton (**1d**$^+$) was first postulated as a transient intermediate for the acid-promoted cleavage of an elongated C–C bond in 1,1,2,2-tetraanisylacenaphthene **2d** to dication **3d**$^{2+}$ (Scheme 6a). Reduction of

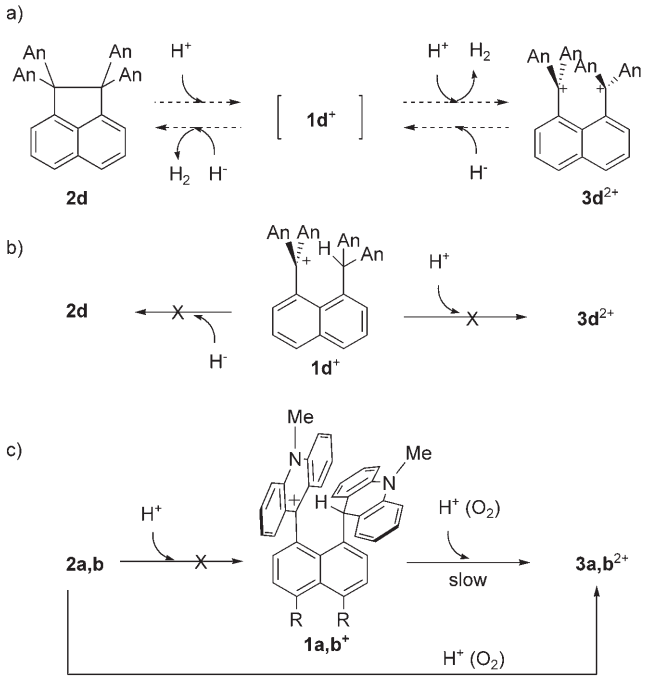

Scheme 6. a) Previously proposed intermediacy of bridged cation **1d**$^+$ during interconversion of **2d** and **3d**$^{2+}$ (ref. [12]); b) Reactivities of isolated salt of **1d**$^+$ (this study); c) Acid-assisted oxidation of **2a** and **2b** and **1a** and **1b**$^+$ (this study).

3d^{2+} with $LiBHEt_3$ was also assumed to form **1d**$^+$, which might be further converted to **2d**. The proposed conversions involve acid-promoted hydride abstraction and hydride-promoted deprotonation steps for the bridged cation **1d**$^+$, which are peculiar types of reactions. Successful isolation of the species in question (**1d**$^+$), as well as its analogues now enables us to experimentally examine whether bridged cations **1**$^+$ exhibit such exotic reactivities as previously proposed by Gabbaï and Wang.[12]

Although **2d** was shown to convert into dication **3d**$^{2+}$ upon treatment with HBF_4, the bridged cation **1d**$^+$ is stable under similar conditions. In fact, treatment with HBF_4/trifluoroacetic anhydride is used to generate **1d**$^+$ from precursor **8d**. Treatment of bridged cation **1d**$^+$ with $NaBH_4$ gave labile hydride adduct **9d** in a high yield (Scheme 7), whereas

 © 2007 Wiley-VCH Verlag GmbH & Co. KGaA, Weinheim

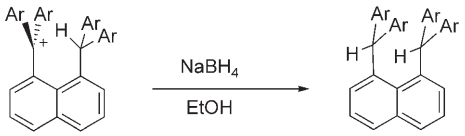

1^+ → **9**

b: Ar_2C=10-methyl-9-acridan; R-R=CH_2-CH_2 (99%)
c: Ar_2C=10-methyl-9-acridan; R-R=CH=CH (61%)
d: Ar=An; R=H (90%)

Scheme 7. Hydride reduction of bridged cations **1b–d**$^+$ to adducts **9b–d**.

$LiBHEt_3$ did not work as well and gave only intractable material. This is also in sharp contrast to the reported reactivity of **3d**$^{2+}$.[12] Thus, it is highly questionable as to whether **1d**$^+$ is involved in the reactions in Scheme 6a. Hydride adducts **9b** and **9c** were also obtained by treating **1b**$^+$ and **1c**$^+$ with $NaBH_4$.

We independently observed acid-promoted fission of extremely long C–C bonds in bis(spiroacridan)-type acenaphthenes **2a** and **2b**, and higher reactivities were observed for **2b** with stronger electron-donating properties. Even a weak Brønsted acid, such as acetic acid, worked effectively to transform **2b** into the corresponding dication **3b**$^{2+}$ (Scheme 6c).[15] When the cleavage reactions of **2a** and **2b** were followed over time by ^{1}H NMR spectroscopy, no resonances assignable to bridged cations **1a**$^+$ and **1b**$^+$ were observed. Another set of experiments indicated that the transformation of **1a**$^+$ and **1b**$^+$ into dications **3a**$^{2+}$ and **3b**$^{2+}$ actually occurred, but the reactions were much slower than for **2a** and **2b** under similar conditions. Furthermore, the conversion of **2a** and **2b** into **3a**$^{2+}$ and **3b**$^{2+}$, respectively, was prevented under deaerated conditions. We concluded that the acid-promoted C–C bond fission of 1,1,2,2-tetraarylacenaphthenes **2** to the dications **3**$^{2+}$ proceeds by acid-assisted oxidation in which molecular oxygen acts as an actual oxidant. This is also the case for the conversion of bridged cations **1**$^+$ to **3**$^{2+}$ under aerated acidic conditions.

Conclusion

The present results demonstrate that intramolecular triarylmethane–triarylmethylium complexes **1a–e**$^+$ with a naphthalene-1,8-diyl-type skeleton can be best described as C–H bridged cations with a localized geometry (form **A**) that exhibit a facile 1,5-hydride shift and a significant degree of CT interaction. As shown by the much larger $\Delta G^{\neq}$ values for a hydride shift in **1b**$^+$ and **1c**$^+$ than in **1a**$^+$, small differences in the geometry of the $[C\cdots H\cdots C]^+$ unit (d_1, d_2, D, and θ) drastically change the behavior of the bridged cations whereas the electronic nature of the cationic unit ($pK_R{}^+$) has little, if any, effect. The latter point was evident when we compared $\Delta G^{\neq}$ values for **1a**$^+$, **1d**$^+$, and **1e**$^+$. This can be explained by considering two counterbalancing electronic factors that increase and decrease the delocalizability of the bridging hydrogen. One is an increase in the hydride-donating properties of a diarylmethane unit in the order **1a**$^+$ > **1d**$^+$ > **1e**$^+$. At the same time, the hydride-accepting properties of the diarylmethylium unit decrease in the same order.

The difference in delocalizability between symmetric $[Si\cdots H\cdots Si]^+$[10a] and unsymmetric $[C\cdots H\cdots C]^+$ can be accounted for mainly by the difference in atomic radii. Changes in electronegativity and the ease of hyperconjugation may also play a role. However, the former may not be important owing to counterbalancing effects, as discussed for a changing $pK_R{}^+$ in the $[C\cdots H\cdots C]^+$ unit. This research shows that studies on isolable triarylmethane–triarylmethylium complexes should provide deeper insight into 3c bonds between carbon and hydrogen, thanks to the finely tunable geometry, the details of which can be determined precisely by X-ray analyses. We are currently studying intramolecular C–H bridged carbocations with much smaller C···H separation (d_1, d_2) by the use of an arylene spacer other than a naphthalene-1,8-diyl-type skeleton.

Experimental Section

General: ^{1}H and ^{13}C NMR spectra were recorded at 300, 400, or 500 MHz and 75, 100, or 125 MHz, respectively, at 23 °C unless indicated otherwise. ^{2}H NMR spectra were recorded at 77 MHz. ^{13}C–^{1}H coupling constants were measured by an HSQC method. IR spectra were recorded in KBr disks. Mass spectra were recorded in the EI mode or the FAB mode. Column chromatography was performed on silica gel of particle size 40–63 μm and aluminum oxide. UV/Vis spectra were measured in spectrograde solvents. 1,8-Dibromonaphthalene,[17] 5,6-dibromoacenaphthene,[19] 5,6-dibromoacenaphthylene,[20] 8-dianisylmethyl-1-naphthoic acid[21] and (8-diphenylmethyl-1-naphthyl)diphenylmethanol[22,23] were prepared following known procedures. Other reagents and solvents were obtained from commercial sources and purified prior to use. Preparation and X-ray analyses of **1a**[OTf] and **1b**[OTf] salts were reported as a preliminary communication.[9a]

Preparation of 1c[OTf]: Methyl triflate (57 μL, 500 μmol) was added to a solution of 9-[6-(10-methylacridan-9-yl)acenaphthylene-5-yl]acridine (**5c**, 26 mg, 50 μmol) in dry benzene (10 mL). After stirring for 40 min at 23 °C under argon, the resulting mixture was filtered and washed with diethyl ether to give **1c**[OTf] (23 mg, 67 %) as a dark green solid. M.p. 215–216 °C; ^{1}H NMR (CD_2Cl_2): δ = 7.91 (br dd, J = 7.0 Hz, 2H), 7.68–7.43 (br m, 10H), 7.30 (s, 2H), 7.11–6.92 (br s, 8H) 4.07–3.90 (br s, 7H); IR (KBr): $\tilde{\nu}$ = 3085, 3032, 2893, 1608, 1588, 1579, 1550, 1479, 1461, 1443, 1386, 1372, 1341, 1272, 1256, 1224, 1193, 1165, 1029, 866, 848, 752, 709, 691, 637, 573, 518 cm^{-1}; UV/Vis (CH_3CN): λ_{max} (ε) = 231 (55600), 263 (69900), 326 (16400), 342 (13900), 358 (12600), 430 nm (5800 M^{-1}cm^{-1}); LR-MS (FAB): m/z (%): 538 (34), 537 ([M]$^+$, 65), 194 (35), 154 (bp), 138 (33), 137 (58), 136 (81); HRMS (FAB): m/z: found: 537.2355; calcd for $C_{40}H_{29}N_2$: 537.2330; elemental analysis calcd (%) for $C_{41}H_{29}F_3N_2O_3S$: C 71.71, H 4.26, N 4.08; found C 72.08, H 4.54, N 3.52.

Other hydrogen-bridged cations **1a**[OTf] and **1b**[OTf] were prepared in a similar manner from **5a** and **5b**, respectively.

1a[OTf]: Yield: 78 %, dark green solid; m.p. 193–195 °C; ^{1}H NMR ([D$_6$]acetone, −30 °C): δ = 8.46 (d, J = 8.1 Hz, 2H), 7.87 (t, J = 7.5 Hz, 2H), 7.72–7.53 (m, 10H), 7.08 (t, J = 7.5 Hz, 4H), 6.98 (d, J = 8.1 Hz, 4H), 4.11 (s, 1H), 4.06 (s, 6H); IR (KBr): $\tilde{\nu}$ = 3107, 3034, 2919, 1609, 1589, 1579, 1549, 1479, 1461, 1342, 1275, 1262, 1224, 1193, 1160, 1030, 774, 753, 713, 691, 655, 637, 629, 517 cm^{-1}; UV/Vis (CH_3CN): λ_{max} (ε) = 221 (71900), 262 (63100), 289 (15000), 344 (7200), 363 (12500), 434 nm (4800 M^{-1}cm^{-1}); LR-MS (FAB): m/z (%): 515 (22), 514 (44), 513 ([M]$^+$, bp), 194 (51); HRMS (FAB): m/z: found: 513.2324; calcd for $C_{38}H_{29}N_2$: 513.2325; elemental analysis calcd (%) for $C_{39}H_{29}F_3N_2O_3S$+0.33 C_6H_6: C 71.50, H 4.54, N 4.07; found: C 71.24, H 4.79, N 3.92.

 © 2007 Wiley-VCH Verlag GmbH & Co. KGaA, Weinheim

1b[OTf]: Yield: 68%, dark green solid; m.p. 248–249°C; ^{1}H NMR ([D$_6$]acetone, −10°C): δ=7.81–7.57 (brs, 8H), 7.64 (d, J=7.0 Hz, 2H), 7.50 (d, J=7.0 Hz, 2H), 7.18–6.94 (brs, 8H), 4.10 (brs, 6H), 4.00 (s, 1H), 3.65 (s, 4H); ^{1}H NMR ([D$_6$]acetone, −85°C): δ=8.98 (d, J=9.4 Hz, 2H), 8.55 (brdd, J=9.4, 7.3 Hz, 2H), 8.15(d, J=8.6 Hz, 2H), 7.99 (brdd, J=8.6, 7.3 Hz, 2H), 7.78 (d, J=7.2 Hz, 1H), 7.68 (d, J=7.2 Hz, 1H), 7.53 (d, J=7.3 Hz, 1H), 7.45 (d, J=7.3 Hz, 1H), 7.03 (brdd, J=8.3, 7.3 Hz, 2H), 6.82 (d, J=8.3 Hz, 2H), 6.50 (t, J=7.3 Hz, 2H), 5.96 (d, J=7.3 Hz, 2H), 5.16 (s, 3H), 4.19 (s, 1H), 3.66 (d, J=8.3 Hz, 4H), 3.25 (s, 3H); IR (KBr): $\tilde{\nu}$=3111, 3070, 3037, 2921, 2888, 1607, 1590, 1577, 1547, 1462, 1385, 1343, 1277, 1262, 1224, 1187, 1155, 1045, 1032, 866, 752, 638, 574, 517 cm^{-1}; UV/Vis (CH_3CN): λ_{max} (ε)=210 (72300), 232 (79700), 262 (84300), 304 (19100), 361 (14100), 426 nm (5500 M^{-1}cm^{-1}); LR-MS (FAB): m/z (%): 540 (45), 539 ([M]$^+$, bp), 194 (51); HRMS (FAB): m/z: found: 539.2484; calcd for $C_{40}H_{31}N_2$: 539.2482.; elemental analysis calcd (%) for $C_{39}H_{29}F_3N_2O_3S$+0.50 H_2O C 70.57, H 4.62, N 4.01; found C 70.69, H 4.61, N 4.09.

Preparation of [D$_1$]1c[OTf]: Methyl triflate (130 μL, 1.1 mmol) was added to a solution of 9-[6-(9-deuterio-10-methylacridan-9-yl)acenaphthylene-5-yl]acridine ([D$_1$]**5c**, 60.0 mg, 115 μmol) in dry benzene (20 mL). After stirring for 20 min at 23°C under argon, the resulting mixture was filtered and washed with diethyl ether to give [D$_1$]**1c**[OTf] as a dark green solid. M.p. 223–225°C; ^{1}H NMR (CD_2Cl_2): δ=7.91 (brdd, J=7.0 Hz, 2H), 7.63–7.40 (br m, 10H), 7.30 (s, 2H), 7.09–6.89 (br s, 8H) 4.08–3.86 (br s, 6H); IR (KBr): $\tilde{\nu}$=3085, 3032, 2970, 2926, 2881, 2822, 1637, 1624, 1608, 1579, 1549, 1462, 1386, 1376, 1339, 1272, 1240, 1224, 1193, 1165, 1151, 1029, 869, 849, 752, 710, 691, 685, 664, 637, 602, 573, 539, 518 cm^{-1}; LR-MS (FAB): m/z (%):539 (30), 538 ([M]$^+$, 59), 154 (bp), 138 (33), 137 (59), 136 (80), 107 (31); HRMS (FAB): m/z: found: 538.2377; calcd for $C_{40}H_{28}DN_2$: 538.2369.

Other deuterium-bridged cations [D$_1$]**1a**[OTf] and [D$_1$]**1b**[OTf] were prepared in a similar manner from [D$_1$]**5a** and [D$_1$]**5b**, respectively.

[D$_1$]1a[OTf]: Yield: 68%, dark green solid; m.p. 193–194°C (decomp); ^{1}H NMR ([D$_6$]acetone): δ=8.46 (d, J=8.3 Hz, 2H), 7.89 (brt, J=7.5 Hz, 2H), 7.70–7.50 (m, 10H), 7.08 (brt, J=7.0 Hz, 4H), 7.00 (d, J=8.1 Hz, 4H), 4.07 (s, 6H); ^{2}D NMR ([D$_6$]acetone, −30°C): δ=4.10 (brs); IR (KBr): $\tilde{\nu}$=3069, 3034, 1609, 1589, 1579, 1549, 1461, 1385, 1341, 1276, 1262, 1224, 1194, 1162, 1030, 753, 713, 691, 654, 637, 626, 602, 573, 517 cm^{-1}; LR-MS (FAB): m/z (%): 517 (32), 516 (26), 515 (85), 514 ([M]$^+$, bp), 513 (29), 195 (48), 136 (27); HRMS (FAB): m/z: found: 514.2388; calcd for $C_{38}H_{28}DN_2$: 514.2392.

[D$_1$]1b[OTf]: Yield: 63%, dark green solid; m.p. 265–267°C (decomp); ^{1}H NMR ([D$_6$]acetone, −85°C): δ=8.98 (d, J=9.4 Hz, 2H), 8.55 (t, J=8.0 Hz, 2H), 8.17 (d, J=8.6 Hz, 2H), 7.99 (t, J=8.0, 2H), 7.78 (d, J=7.2 Hz, 1H), 7.68 (d, J=7.2 Hz, 1H), 7.53 (d, J=7.3 Hz, 1H), 7.45 (d, J=7.3 Hz, 1H), 7.03 (t, J=7.7 Hz, 2H), 6.82 (d, J=8.3 Hz, 2H), 6.50 (t, J=7.3 Hz, 2H), 5.96 (d, J=7.2 Hz, 2H), 5.16 (s, 3H), 3.67 (brs, 4H), 3.25 (s, 3H); ^{2}D NMR ([D$_6$]acetone, −10°C): δ=3.99 (brs); IR (KBr): $\tilde{\nu}$=3113, 3070, 3037, 2932, 2883, 1607, 1591, 1577, 1547, 1464, 1344, 1279, 1262, 1224, 1189, 1157, 1029, 874, 751, 636, 516 cm^{-1}; LR-MS (FAB): m/z (%): 541 (45), 514 ([M]$^+$, bp), 195 (47); HRMS (FAB): m/z: found: 540.2568; calcd for $C_{40}H_{30}DN_2$: 540.2549.

Preparation of 1d[BF$_4$]: Aqueous HBF_4 (40%, 265 μL, 1.74 mmol) was added to a solution of carbinol **8d** (101 mg, 174 μmol) in dry CH_2Cl_2/trifluoroacetic anhydride (5 mL/500 μL). After stirring for 20 min, the mixture was diluted with diethyl ether, and the resulting precipitates were filtered and washed with diethyl ether to give **1d**[BF_4] (55 mg, 47%) as a dark red solid. M.p. 195–196°C; ^{1}H NMR (CD_2Cl_2): δ=8.19 (d, J=7.7 Hz, 2H), 7.61 (dd, J=7.7, 7.3 Hz, 2H), 7.26 (dd, J=7.3, 1.1 Hz, 2H), 6.89 (d, J=8.8 Hz, 8H), 6.81 (d, J=8.8 Hz, 8H), 5.47 (s, 1H), 3.90(s, 12H); IR (KBr): $\tilde{\nu}$=2935, 2836, 1605, 1578, 1508, 1443, 1365, 1318, 1279, 1252, 1161, 1123, 1092, 1056, 1031, 998, 912, 849, 832, 814, 804, 791, 770, 623, 595, 584, 563, 540, 521 cm^{-1}; UV/Vis (CH_3CN): λ_{max} (ε)=226 (58400), 266 (12700), 282 (11300), 339 (7900), 490 nm (40700 M^{-1}cm^{-1}); LR-MS (FAB): m/z (%):580 (44), 579 ([M]$^+$, bp), 307 (15), 289(11), 227 (13), 155 (14), 154 (60), 138 (16), 137 (30), 136 (45), 107 (12), 77 (11); HRMS (FAB): m/z: found: 579.2548; calcd for $C_{40}H_{35}O_4$: 579.2535; elemental analysis calcd (%) for $C_{40}H_{35}O_4BF_4$+0.5 H_2O: C 71.12, H 5.37; found C 71.07, H 5.30.

Preparation of 1e[BF$_4$]: Aqueous HBF_4 (40%, 100 μL, 640 μmol) was added to a solution of (8-diphenylmethyl-1-naphthyl)diphenylmethanol[23] (30 mg, 62.9 μmol) in dry CH_2Cl_2/trifluoroacetic anhydride (3 mL/500 μL). After stirring for 10 min at 23°C, the mixture was diluted with dry diethyl ether and the resulting precipitates were filtered and washed with diethyl ether to give **1e**[BF_4] (12.7 mg, 37%) as a dark green solid. M.p. 198–199°C; ^{1}H NMR (CD_2Cl_2): δ=8.42 (dd, J=8.1, 1.4 Hz, 2H), 7.71 (dd, J=8.1, 7.5 Hz, 2H), 7.65 (t, J=7.9 Hz, 4H), 7.37 (t, J=7.9 Hz, 8H), 7.31 (dd, J=7.5, 1.4 Hz, 2H), 6.82 (d, J=7.9 Hz, 8H), 5.30 (s, 1H); IR (KBr): $\tilde{\nu}$=3068, 3022, 2847, 1578, 1552, 1497, 1480, 1451, 1443, 1425, 1389, 1351, 1322, 1281, 1238, 1210, 1186, 1088, 1051, 994, 791, 768, 754, 736, 710, 698, 671, 552 cm^{-1}; UV/Vis (CH_3CN): λ_{max} (ε)=212 (55200, sh), 234 (28700, sh), 337 (6800), 400 (16900), 587 nm (9600 M^{-1}cm^{-1}); LR-MS (FAB): m/z (%):460 (43), 439 ([M]$^+$, bp), 458 (13), 291 (12), 289 (16), 215 (14), 167 (43), 165 (16), 154 (37), 137 (19), 136 (31); HRMS (FAB): m/z: found: 459.2106; calcd for $C_{36}H_{27}$: 459.2113; elemental analysis calcd (%) for $C_{36}H_{27}BF_4$+0.5 H_2O: C 77.85, H 5.08; found C 77.73, H 5.07.

Preparation of 4c: CuO (600 mg, 7.54 mmol) and [Pd(PPh$_3$)$_4$] (1.15 g, 995 μmol) were added to a solution of 5,6-dibromoacenaphthylene (1.02 g, 3.30 mmol) in dry DMF (100 mL). After bubbling with argon for 30 min, the mixture was heated at 140°C under argon. After 5 min, a solution of 9-trimethylstannylacridine (**13**, 4.52 g, 13.2 mmol) in dry DMF (20 mL) was added at this temperature. After 21 h, 5% aqueous ammonium hydroxide (100 mL) and hexane (200 mL) were added to the reaction mixture. The resulting precipitates were filtered. The filtered solid was extracted with $CHCl_3$, and the extract was washed with brine and then dried over Na_2SO_4. The black solid obtained by evaporation of the solvent was purified by chromatography (SiO_2, $CHCl_3$/Et_3N 100:1) to give **4c** (674 mg, 40%) as a yellow solid. M.p. 255–258°C (decomp); ^{1}H NMR ($CDCl_3$): δ=7.91 (dd, J=6.9, 1.1 Hz, 2H), 7.71 (dd, J=8.6, 0.6 Hz, 4H), 7.38–7.33 (m, 8H), 6.96 (dd, J=8.6, 0.6 Hz, 4H), 6.70 (ddd, J=8.6, 6.9, 1.1 Hz, 4H); ^{13}C NMR ($CDCl_3$): δ=146.70, 144.87, 140.88, 134.70, 131.86, 130.08, 129.34, 129.31, 129.07, 128.87, 126.15, 124.85, 124.74, 124.20; IR (KBr): $\tilde{\nu}$=3070, 1556, 1540, 1515, 1460, 1436, 1408, 1154, 1011, 869, 752, 688, 603 cm^{-1}; UV/Vis (CH_2Cl_2): λ_{max} (ε)=329 (15400), 348 (17400), 360 (16700), 390 nm (7400 M^{-1}cm^{-1}, sh); fluorescence (CH_2Cl_2, λ_{ex} 360 nm): λ_{max}=530 nm; LR-MS (EI) m/z (%): 507 (42), 506 ([M]$^+$, bp), 253 (21), 252 (14); HRMS (EI): m/z: found: 506.1789; calcd for $C_{38}H_{22}N_2$: 506.1783; elemental analysis calcd (%) for $C_{38}H_{22}N_2$+0.25 $CHCl_3$: C 85.64, H 4.18, N5.22; found C 85.20, H 4.32, N 5.10.

Other diacridines **4a** and **4b** were prepared in a similar manner from 1,8-dibromonaphthalene and 5,6-dibromoacenaphthene, respectively.

4a: Yield: 23%, yellow solid; m.p. 245–247°C (decomp); ^{1}H NMR (CD_2Cl_2): δ=8.24 (dd, J=8.4, 1.4 Hz, 2H), 7.67 (dd, J=8.4, 6.9 Hz, 2H), 7.52 (dd, 4H, J=8.4, 1.2 Hz), 7.29 (ddd, J=8.4, 6.6, 1.4 Hz, 4H), 7.19 (dd, J=6.9, 1.4 Hz, 2H), 6.72 (dd, J=8.4, 1.4 Hz, 4H), 6.61 (ddd, J=8.4, 6.6, 1.2 Hz, 4H). The ^{13}C NMR could not be measured owing to the low solubility of **4a**. IR (KBr): $\tilde{\nu}$=3045, 1558, 1540, 1517, 1436, 1145, 1014, 866, 827, 785, 752, 601 cm^{-1}; UV/Vis (CH_2Cl_2): λ_{max} (ε)=347 (12600), 360 (13400), 390 nm (6000 M^{-1} cm^{-1}, sh); fluorescence (CH_2Cl_2, λ_{ex} 360 nm) λ_{max}=536 nm; LR-MS (EI): m/z (%): 484 ([M]$^+$+2H, 57), 483(23), 482([M]$^+$, bp), 241(87), 240 (65), 207 (66), 196 (60), 171 (63), 166 (64), 138 (63), 122 (61), 121 (63), 93 (64), 80 (63), 52 (58); HRMS (EI): m/z: found: 482.1778; calcd for $C_{36}H_{22}N_2$: 482.1783; elemental analysis calcd (%) for $C_{36}H_{22}N_2$+0.50 $CHCl_3$: C 80.84, H 4.18, N 5.17; found C 80.88, H 4.48, N 5.20.

4b: Yield: 48%, yellow solid; m.p. 270–272°C (decomp); ^{1}H NMR ($CDCl_3$): δ=7.69 (d, J=8.4 Hz, 4H), 7.55 (d, J=7.0 Hz, 2H), 7.34 (ddd, J=8.4, 6.4, 1.1 Hz, 4H), 7.25 (d, J=7.0 Hz, 2H), 6.94 (dd, J=8.6, 1.1 Hz, 4H), 6.68 (ddd, J=8.6, 6.4, 1.1 Hz, 4H), 3.74 (s, 4H); ^{13}C NMR ($CDCl_3$): δ=147.55, 146.71, 145.89, 140.28, 131.92, 131.76, 128.93, 128.79, 126.25, 124.94, 124.57, 119.50, 30.51; IR (KBr): $\tilde{\nu}$=3042, 2916, 1629, 1600, 1556, 1515, 1460, 1435, 1408, 1329, 1151, 1013, 868, 745, 647, 626, 603 cm^{-1}; UV/Vis (CH_2Cl_2): λ_{max} (ε)=349 (12200), 360 (12900), 390 nm (6200 M^{-1}cm^{-1}, sh); fluorescence (CH_2Cl_2, λ_{ex} 360 nm) λ_{max}=525 nm; LR-MS (EI): m/z (%): 509 (42), 508 ([M]$^+$, bp), 254 (19); HRMS (EI): m/z:

 © 2007 Wiley-VCH Verlag GmbH & Co. KGaA, Weinheim

found: 508.1940; calcd for $C_{38}H_{24}N_2$: 508.1939; elemental analysis calcd (%) for $C_{38}H_{24}N_2+0.33\,H_2O$: C 88.69, H 4.83, N 5.44; found C 88.42, H 4.75, N 5.41.

Preparation of 5c: A solution of methyl triflate in dry benzene (0.22 M, 1.0 mL, 220 μmol) was added to a solution of 9,9′-(acenaphthylene-5,6-diyl)diacridine (**4c**, 88.9 mg, 175 μmol) and 2,6-di-*tert*-butyl-4-methylpyridine (35.8 mg, 175 μmol) in dry benzene (100 mL). The whole mixture was stirred for 22.5 h at 23 °C under argon, and the resulting orange precipitates were filtered to give monomethylated acridinium OTf^- salt accompanied by a small amount of dimethylated dication salt $\mathbf{3c}^{2+}(OTf^-)_2$ and pyridinium triflate. The mixture was used in the next reaction without further purification. $NaBH_4$ (110 mg, 2.9 mmol) was added to a suspension of the above mixture containing monoacridinium OTf^- salt in EtOH (30 mL). After stirring for 20 min at 23 °C, the solvent was evaporated. The resulting yellow solid was suspended in water, and the mixture was extracted with CH_2Cl_2. The organic layers were combined and then washed with brine, dried over Na_2SO_4, and filtered. The yellow solid obtained by evaporation of the solvent was purified by chromatography (Al_2O_3, CH_2Cl_2/*n*-hexane 1:1) to give **5c** (69 mg, 75%) as a yellow solid. M.p. 220–223 °C (decomp); ^{1}H NMR ($CDCl_3$): $\delta=8.18$ (d, $J=8.1$ Hz, 2H), 7.86 (d, $J=7.0$ Hz, 1H), 7.68 (d, $J=7.0$ Hz, 2H), 7.62 (d, $J=8.1$ Hz, 2H), 7.49 (d, $J=7.0$ Hz, 2H), 7.32–7.22 (m, 3H), 7.17 (s, 2H), 6.91 (t, $J=7.7$ Hz, 2H), 6.59 (d, $J=8.1$ Hz, 2H), 6.40 (t, $J=7.5$ Hz, 2H), 6.05 (d, $J=7.5$ Hz, 2H), 4.43 (s, 1H) 3.16 (s, 3H); ^{13}C NMR ($CDCl_3$): $\delta=148.64$, 141.50, 141.20, 138.86, 133.57, 133.29, 132.60, 132.19, 130.13, 129.48, 128.74, 128.69, 128.10, 127.46, 126.48, 126.02, 125.69, 125.59, 123.32, 119.51, 115.82, 111.63, 42.48, 32.97; IR (KBr): $\tilde{\nu}=3056$, 3029, 2958, 2877, 2826, 1607, 1592, 1556, 1515, 1479, 1436, 1407, 1355, 1318, 1286, 1267, 1131, 865, 838, 760, 743, 674 cm^{-1}; LR-MS (EI) *m*/*z* (%):524 (19), 523 (45), 522 ([*M*]$^+$, bp), 521 (26), 508 (20), 507 (47), 262 (12), 261 (28), 194 (28); HRMS (EI): *m*/*z*: found: 522.2094; calcd for $C_{39}H_{26}N_2$: 522.2096; elemental analysis calcd (%) for $C_{39}H_{26}N_2+0.33\,EtOH$: C 88.56, H 5.25, N 5.21; found C 88.50, H 5.60, N 5.25.

Other acridan–acridine hybrids **5a** and **5b** were prepared in a similar manner from **4a** and **4b**, respectively.

5a: Yield: 77%, yellow solid; m.p. 280–285 °C (decomp); ^{1}H NMR ($CDCl_3$): $\delta=8.16$ (dd, $J=8.4$, 1.2 Hz, 1H), 8.08 (d, $J=8.8$ Hz, 2H), 8.03 (dd, $J=8.0$, 1.5 Hz, 1H), 7.65 (dd, $J=8.0$, 7.2 Hz, 1H), 7.61–7.54 (m, 3H), 7.49 (dd, $J=7.2$, 1.5 Hz, 1H), 7.45 (dd, $J=8.4$, 0.6 Hz, 2H), 7.41 (dd, $J=6.6$, 1.2 Hz, 1H), 7.15 (ddd, $J=8.4$, 6.6, 1.2 Hz, 2H), 6.87 (td, $J=7.5$, 1.2 Hz, 2H), 6.48 (dd, $J=7.5$, 1.2 Hz, 2H), 6.40 (dd, $J=7.5$, 1.2 Hz, 2H), 6.10 (dd, $J=7.5$, 1.2 Hz, 2H), 4.52 (s, 1H), 3.04 (s, 3H); ^{13}C NMR ($CDCl_3$): $\delta=148.95$, 148.57, 141.74, 140.16, 135.19, 132.90, 132.60, 132.08, 131.32, 130.79, 129.96, 129.57, 129.10, 128.66, 128.08, 127.19, 127.06, 126.36, 126.19, 125.19, 124.43, 119.41, 111.04, 43.07, 32.96; IR (KBr): $\tilde{\nu}=$ 3059, 3037, 2960, 2926, 1589, 1503, 1477, 1456, 1359, 1322, 1273, 781, 744 cm^{-1}; LR-MS (EI): *m*/*z* (%): 500 (20), 499 (46), 498 ([*M*]$^+$, bp), 497 (24), 496 (22), 484 (27), 483 (55), 249 (28), 194 (48); HRMS (EI): *m*/*z*: found: 498.2096; calcd for $C_{37}H_{26}N_2$: 498.2096; elemental analysis calcd (%) for $C_{37}H_{26}N_2+0.25\,H_2O$: C 88.33, H 5.31, N 5.57; found C 88.40, H 5.55, N 5.35.

5b: Yield: 95%, yellow solid; m.p. 220–223 °C (decomp); ^{1}H NMR ($CDCl_3$): $\delta=8.16$ (dd, $J=8.6$, 1.2 Hz, 2H), 7.65–7.58 (m, 4H), 7.46 (d, $J=$ 7.2 Hz, 1H), 7.40 (d, $J=7.5$ Hz, 1H), 7.36 (d, $J=7.2$ Hz, 1H), 7.32 (d, $J=$ 7.5 Hz, 1H), 7.24 (dd, $J=8.6$, 7.2 Hz, 2H), 6.87 (tt, $J=8.1$, 0.6 Hz, 2H), 6.54 (d, $J=8.1$ Hz, 2H), 6.39 (t, $J=7.5$ Hz, 2H), 6.07 (d, $J=7.5$, 1.1 Hz, 2H), 4.35 (s, 1H), 3.60–3.48 (m, 4H), 3.10 (s, 3H); ^{13}C NMR (CD_2Cl_2): $\delta=148.58$ (br), 148.19, 145.58, 141.24, 139.97, 132.23, 132.69, 132.22, 129.77, 129.35 (br), 127.90, 127.70, 127.40, 127.28, 126.15, 125.61, 125.25, 120.47, 119.11, 118.31, 111.51, 41.80, 32.65, 30.05, 29.76; IR (KBr): $\tilde{\nu}=$ 1606, 1590, 1461, 1346, 1266, 1131, 866, 752 cm^{-1}; LR-MS (EI): *m*/*z* (%): 525 (64), 524 ([*M*]$^+$, bp), 523 (49), 510 (52), 509 (69), 328 (53), 262 (40), 194 (51), 179 (50); HRMS (EI): *m*/*z*: found: 524.2257; calcd for $C_{39}H_{28}N_2$: 524.2252; elemental analysis calcd (%) for $C_{39}H_{28}N_2+0.50\,H_2O$: C 86.32, H 5.57, N5.16; found C 86.06, H 5.43, N 5.12.

Deuterated compounds [D_1]**5a–c** were prepared in a similar manner to **4a–c**, respectively, by using $NaBD_4$ instead of $NaBH_4$.

[D_1]5a: Yield: 41%, yellow solid; m.p. 270–271 °C (decomp); ^{1}H NMR ($CDCl_3$): $\delta=8.16$ (dd, $J=8.4$, 1.2 Hz, 1H), 8.07 (d, $J=8.8$ Hz, 2H), 8.03 (dd, $J=8.0$, 1.5 Hz, 1H), 7.64 (dd, $J=8.0$, 7.2 Hz, 1H), 7.60–7.53 (m, 3H), 7.49 (dd, $J=7.2$, 1.5 Hz, 1H), 7.44 (d, $J=8.6$ Hz, 2H), 7.40 (dd, $J=$ 6.6, 1.2 Hz, 1H), 7.14 (ddd, $J=8.6$, 6.6, 1.1 Hz, 2H), 6.86 (td, $J=7.5$ 1.5 Hz, 2H), 6.48 (d, $J=7.5$ Hz, 2H), 6.40 (dt, $J=7.5$, 1.1 Hz, 2H), 6.10 (dd, $J=7.5$, 1.5 Hz, 2H), 3.04 (s, 3H); ^{13}C NMR ($CDCl_3$): $\delta=148.91$, 148.62, 141.78, 140.07, 135.22, 132.90, 132.56, 132.13, 131.30, 130.78, 129.92, 129.16, 128.66, 128.03, 127.19, 127.05, 126.36, 126.20, 125.24, 125.19, 124.44, 119.42, 111.05, 32.95; IR (KBr): $\tilde{\nu}=3056$, 2958, 2926, 2872, 1625, 1605, 1589, 1556, 1539, 1514, 1459, 1439, 1343, 1301, 1261, 1209, 1200, 1160, 1144, 1129, 1045, 862, 783, 776, 746, 651, 638, 618, 601 cm^{-1}; LR-MS (EI): *m*/*z* (%): 500 (43), 499([*M*]$^+$, bp), 498 (20), 484 (29), 250 (27), 195 (30); HRMS (EI): *m*/*z*: found: 499.2163; calcd for $C_{37}H_{25}DN_2$: 499.2158.

[D_1]5b: Yield: 77%, yellow solid; m.p. 233–235 °C (decomp); ^{1}H NMR ($CDCl_3$): $\delta=8.14$ (d, $J=8.6$ Hz, 2H), 7.67–7.58 (m, 4H), 7.47 (d, $J=$ 6.9 Hz, 1H), 7.41 (d, $J=7.2$ Hz, 1H), 7.36 (d, $J=7.2$ Hz, 1H), 7.32 (d, $J=$ 6.9 Hz, 1H), 7.24 (m, 2H), 6.88 (td, $J=7.8$, 1.5 Hz, 2H), 6.54 (d, $J=$ 7.8 Hz, 2H), 6.40 (td, $J=7.8$, 0.6 Hz, 2H), 6.08 (dd, $J=7.8$, 1.5 Hz), 3.61–3.52 (m, 4H), 3.12 (s, 3H); ^{13}C NMR ($CDCl_3$): $\delta=148.82$, 148.74, 148.06, 145.46, 141.64, 140.19, 137.87, 133.11, 132.50, 130.67, 129.97, 129.38, 128.06, 127.76, 127.51, 126.23, 125.86, 125.26, 120.84, 119.40, 118.46, 111.35, 32.94, 30.32, 30.07; IR (KBr): $\tilde{\nu}=3070$, 3037, 2924, 2854, 1605, 1592, 1514, 1470, 1435, 1345, 1278, 1269, 1132, 874, 757, 751 cm^{-1}; LR-MS (EI): *m*/*z* (%): 526 (50), 525 ([*M*]$^+$, bp), 524 (28), 510 (28), 278 (39), 263 (36), 195 (28); HRMS (EI): *m*/*z*: found: 525.2318; calcd for $C_{39}H_{27}DN_2$: 525.2314.

[D_1]5c: Yield: 63%, yellow solid; m.p. 245–248 °C (decomp); ^{1}H NMR ($CDCl_3$): $\delta=8.17$ (dd, $J=8.8$ Hz, 2H), 7.81 (dd, $J=7.0$, 1.1 Hz, 1H), 7.66 (d, $J=8.1$ Hz, 2H), 7.61 (d, $J=7.9$ Hz, 2H), 7.47 (dd, $J=7.0$, 1.1 Hz, 2H), 7.30–7.20 (m, 3H), 7.13 (s, 2H), 6.88 (t, $J=7.7$ Hz, 2H), 6.56 (d, $J=$ 8.1 Hz, 2H), 6.38 (t, $J=7.5$ Hz, 2H), 6.03 (d, $J=7.7$ Hz, 2H), 2.98 (s, 3H); ^{13}C NMR ($CDCl_3$): $\delta=148.60$, 147.75, 144.86, 141.47, 141.17, 138.83, 133.54, 132.48, 132.15, 130.09, 129.61, 129.47, 128.72, 128.66, 128.07, 127.90, 127.49, 127.44, 126.47, 126.00, 125.66, 125.58, 123.29, 119.49, 111.63, 32.92; IR (KBr): $\tilde{\nu}=3274$, 3059, 2958, 2918, 2873, 1609, 1591, 1515, 1470, 1437, 1407, 1356, 1271, 1132, 865, 854, 760, 743, 674 cm^{-1}; LR-MS (EI): *m*/*z* (%):525 (11), 524 (41), 523 ([*M*]$^+$, bp), 522 (29), 509 (17), 508 (40) 262 (13), 262 (30), 195 (31), 149 (23); HRMS (EI): *m*/*z*: found: 523.2149; calcd for $C_{39}H_{25}DN_2$: 523.2158.

Preparation of 8d: A solution of 8-dianisylmethyl-1-naphthoic acid (660 mg, 1.5 mmol)[21] in THF (50 mL) was treated with an excess amount of a solution of CH_2N_2 in diethyl ether. The solution was evaporated to afford ester **7d**. A solution of anisyllithium in THF, which was generated from anisyl iodide (1.26 g, 5.4 mmol) and *n*-butyl lithium (1.59 M in *n*-hexane, 3.4 mL, 5.4 mmol) at −78 °C, was added to a solution of ester **7d** (371 mg, 899 μmol) in dry diethyl ether (40 mL). The mixture was allowed to warm to 23 °C and stirred for 18 h. The mixture was diluted with water and extracted with diethyl ether. The organic layer was washed with brine, dried over $MgSO_4$, and evaporated. The crude product was purified by chromatography (Al_2O_3) to give carbinol **8d** (397 mg, 76%) as a pale yellow solid. M.p. 114–116 °C; ^{1}H NMR ($CDCl_3$): $\delta=7.77$ (dd, $J=8.1$, 1.4 Hz, 1H), 7.76 (dd, $J=8.1$, 1.4 Hz, 1H), 7.36 (d, $J=7.5$ Hz, 1H) 7.17 (d, $J=8.1$ Hz, 1H), 7.14 (d, $J=7.5$ Hz, 1H), 6.89 (dd, $J=7.5$, 1.4 Hz, 1H), 6.83 (s, 1H), 6.73 (d, $J=8.8$ Hz, 4H), 6.58 (d, $J=8.8$ Hz, 4H), 6.41 (d, $J=8.1$ Hz, 4H), 3.78 (s, 6H), 3.71 (s, 6H), 3.28 (s, 1H); IR (KBr): $\tilde{\nu}=3493$, 3062, 3037, 2998, 2951, 2906, 2834, 1727, 1607, 1582, 1509, 1463, 1442, 1301, 1250, 1177, 1111, 1036, 823, 779, 770, 587, 554 cm^{-1}; LR-MS (FD): *m*/*z* (%):595 ([*M*]$^+$, 6), 580 (13), 579 (54), 578 (bp); elemental analysis calcd (%) for $C_{40}H_{37}O_5$: C 80.51, H 6.08; found C 80.54, H 6.28.

Reaction of the bridged cation with hydride—formation of 9b: $NaBH_4$ (46 mg, 1.2 mmol) was added to a solution of **1b[OTf]** (7.7 mg, 11.2 μmol) in EtOH (10 mL). After stirring for 4 h at 23 °C, the solvent was evaporated. The resulting yellow solid was suspended in water and extracted with CH_2Cl_2. The organic layers were combined and then washed with brine, dried over Na_2SO_4, and filtered. The yellow solid ob-

 © 2007 Wiley-VCH Verlag GmbH & Co. KGaA, Weinheim

tained by evaporation of the solvent was purified by chromatography (Al_2O_3, CH_2Cl_2/*n*-hexane 1:1) to give **9b** (6.0 mg, 99%) as a white solid. M.p. 228–230°C (decomp); ^{1}H NMR ($CDCl_3$): δ=7.43 (d, J=7.5 Hz, 2H), 7.36 (d, J=7.5 Hz, 2H), 6.90 (t, J=7.5 Hz, 2H), 6.58 (d, J=7.5 Hz, 2H), 6.47 (d, J=8.8 Hz, 2H), 6.42 (t, J=7.5 Hz, 2H), 6.36 (t, J=8.8 Hz, 4H), 6.13 (d, J=7.5 Hz, 2H), 6.09 (d, J=7.5 Hz, 2H), 5.77(s, 1H), 5.44 (s, 1H), 3.55(s, 4H), 3.21(s, 3H), 3.18 (s, 3H); ^{13}C NMR ($CDCl_3$): δ= 147.71, 146.23, 142.77, 142.33, 140.12, 136.15, 134.56, 131.78, 131.74, 131.57, 130.00, 128.34, 127.14, 126.79, 126.48, 126.43, 125.31, 120.05, 119.42, 118.94, 110.84, 110.00, 51.16, 45.26, 33.28, 33.22, 30.27, 29.85; IR (KBr): $\tilde{\nu}$=3082, 3032, 2924, 2855, 2365, 1726, 1636, 1608, 1590, 1468, 1347, 1267, 1130, 1050, 868, 747 cm^{-1}; LR-MS (EI): *m*/*z* (%):542 (17), 541 (52), 540 ([*M*]$^+$, bp), 526 (23), 525 (43), 347 (13), 346 (35), 270 (13), 194 (38); HRMS (EI): *m*/*z*: found: 540.2570; calcd for $C_{40}H_{32}N_2$: 540.2565; elemental analysis calcd (%) for $C_{40}H_{32}N_2$+CH_2Cl_2: C78.71, H 5.48, N 4.48; found C 78.42, H 5.84, N 4.50.

Other bis(diarylmethyl) derivatives **9c**,**d** were formed upon treatment of the salts of **1c**,**d[OTf]** with $NaBH_4$ in a similar manner.

9c: Yield: 61%, yellow solid; m.p. 245–247°C (decomp); ^{1}H NMR ($CDCl_3$): δ=7.74 (d, J=6.8 Hz, 1H), 7.73 (d, J=7.2 Hz, 1H), 7.53 (d, 1H, J=6.8 Hz), 7.42 (d, J=7.2 Hz, 1H), 7.15 (d, J=1.0 Hz, 2H), 6.92 (t, J=7.5 Hz, 2H), 6.58 (t, J=7.5 Hz, 2H), 6.50 (d, J=7.5 Hz), 6.43 (t, J= 7.5 Hz, 2H), 6.36 (t, J=7.5 Hz, 2H), 6.14 (d, J=7.5 Hz, 2H), 6.10 (d, J= 7.5 Hz, 2H), 5.82 (s, 1H), 5.52 (s, 1H), 3.21 (s, 3H), 3.20 (s, 3H);^{13}C NMR ($CDCl_3$): δ=142.65, 141.15, 139.95, 138.78, 138.45, 135.57, 134.15, 129.73, 129.33, 128.36, 127.29, 126.75, 126.60, 125.54, 124.41, 124.24, 120.10, 119.53, 110.89, 110.15, 51.15, 45.58, 33.27; IR (KBr): $\tilde{\nu}$= 3068, 3029, 2964, 2871, 2809, 1606, 1589, 1496, 1465, 1430, 1346, 1305, 1266, 1182, 1166, 1129, 1092, 1050, 864, 842, 743, 678, 656 cm^{-1}; LR-MS (EI): *m*/*z* (%):540 (16), 539 (45), 538 ([*M*]$^+$, bp), 525 (10), 524 (29), 523 (66), 522 (18), 521 (10), 507 (14), 344 (26), 269 (12), 195 (10), 194 (56), 179 (12); HRMS (EI): *m*/*z*: found: 538.2384; calcd for $C_{40}H_{30}N_2$: 538.2409; elemental analysis calcd (%) for $C_{40}H_{30}N_2$: C 89.19, H 5.61, N 5.20; found C 89.20, H 5.68, N 5.16.

9d: Yield: 90%, pale yellow solid; m.p. 196–198°C (decomp); ^{1}H NMR (C_6D_6): δ=7.65 (d, J=6.8 Hz, 2H), 7.40 (dd, J=7.7, 6.8 Hz, 2H), 7.19 (d, 2H, J=7.7 Hz), 6.92 (d, J=8.8 Hz, 8H), 6.76 (s, 2H), 6.70 (d, J=8.8 Hz, 8H), 3.26 (s, 12H); IR (KBr): $\tilde{\nu}$=3001, 2953, 2929, 2907, 2835, 1606, 1582, 1508, 1462, 1442, 1299, 1247, 1176, 1110, 1034, 857, 838, 821, 803, 781, 767, 584, 534 cm^{-1}; LR-MS (FD): *m*/*z* (%):581 (44), 580 ([*M*]$^+$, bp); HRMS (FD): *m*/*z*: found: 580.2632; calcd for $C_{40}H_{36}O_4$: 580.2614; elemental analysis calcd (%) for $C_{40}H_{36}O_4$+H_2O: C 80.24, H 6.40; found C 79.97, H 6.25.

X-ray analysis:CCDC 288334 (**1a**[OTf]·acetone), CCDC 288335 (**1b**-[OTf]·$CHCl_3$), CCDC 648371 (**1c**[OTf]·$CHCl_3$), CCDC 648372 (**1d**[BF_4]), CCDC 648373 (**1e**[BF_4]) contain the supplementary crystallographic data for this paper. These data can be obtained free of charge from the Cambridge Crystallographic Data Centre via www.ccdc.cam.ac.uk/data_request/cif.

Crystal data for ***1a[OTf]·acetone***: Formula $C_{43}H_{35}F_3N_2O_4S$, M_w 720.80, dark orange plates, 0.60×0.03×0.02 mm^3, triclinic $P\bar{1}$, a=8.407(4) Å, b= 13.578(7) Å, c=15.815(8) Å, α=72.28(2)°, β=80.88(2)°, γ=89.70(3)°, V=1695.9(14) Å^3, ρ(Z=2)=1.411 g cm^{-3}. A total of 6566 unique data ($2\theta_{max}$=55°) were measured at T=133 K by a CCD apparatus ($Mo_{K\alpha}$ radiation, λ=0.71070 Å). Numerical absorption correction was applied (μ= 1.60 cm^{-1}). The structure was solved by the Patterson method and the following expansion (DIRDIF99) and refined by the full-matrix least-squares method on F^2 with anisotropic temperature factors for non-hydrogen atoms. All of the hydrogen atoms, except for the methine proton, were located at the calculated positions and refined with riding. The methine proton was located in the D map and refined with isotropic temperature factors. The final R1 and wR2 values are 0.081 (I>2σI) and 0.197 (all data) for 6555 reflections and 508 parameters.

Crystal data for ***1b[OTf]·CHCl$_3$***: Formula $C_{43}H_{32}Cl_3F_3N_2O_3S$, M_w 808.14, dark brown plates, 0.70×0.20×0.02 mm^3, triclinic $P\bar{1}$, a=8.208(2) Å, b= 14.152(4) Å, c=16.716(5) Å, α=109.750(5)°, β=97.638(5)°, γ= 90.402(3)°, V=1808.4(9) Å^3, ρ(Z=2)=1.484 g cm^{-3}. A total of 7678 unique data ($2\theta_{max}$=55°) were measured at T=103 K by a CCD apparatus ($Mo_{K\alpha}$ radiation, λ=0.71070 Å). Numerical absorption correction was applied (μ=3.71 cm^{-1}). The structure was solved by the direct method (SIR97) and refined by the full-matrix least-squares method on F^2 with anisotropic temperature factors for non-hydrogen atoms. All of the hydrogen atoms, except for the methine proton, were located at the calculated positions and refined with riding. The methine proton was located in the D map and refined with isotropic temperature factors. The final R1 and wR2 values are 0.054 (I>2σI) and 0.128 (all data) for 7678 reflections and 522 parameters.

Crystal data for ***1c[OTf]·CHCl$_3$***: Formula $C_{42}H_{30}Cl_3F_3N_2O_3S$, M_w 806.12, yellow plates, 0.70×0.20×0.02 mm^3, triclinic $P\bar{1}$, a=8.288(3) Å, b= 13.908(6) Å, c=16.579(7) Å, α=109.844(6)°, β=97.679(7)°, γ= 90.430(7)°, V=1778.5(12) Å^3, ρ(Z=2)=1.528 g cm^{-3}. A total of 7842 unique data ($2\theta_{max}$=55°) were measured at T=93 K by a CCD apparatus ($Mo_{K\alpha}$ radiation, λ=0.71070 Å). Numerical absorption correction was applied (μ=3.781 cm^{-1}). The structure was solved by the direct method (SIR97) and refined by the full-matrix least-squares method on F^2 with anisotropic temperature factors for non-hydrogen atoms. All of the hydrogen atoms, except for the methine proton, were located at the calculated positions and refined with riding. The methine proton was located in the D map and refined with isotropic temperature factors. The final R1 and wR2 values are 0.077 (I>2σI) and 0.252 (all data) for 7842 reflections and 520 parameters.

Crystal data for ***1d[BF$_4$]***: Formula $C_{40}H_{35}F_4O_4B$, M_w 666.52, red blocks, 0.20×0.10×0.05 mm^3, monoclinic $P2_1/c$, a=16.434(4) Å, b=14.951(3) Å, c=27.399(7) Å, β=102.634(6)°, V=6569(3) Å^3, ρ(Z=8)=1.348 g cm^{-3}. A total of 14911 unique data ($2\theta_{max}$=55°) were measured at T=123 K by a CCD apparatus ($Mo_{K\alpha}$ radiation, λ=0.71070 Å). Numerical absorption correction was applied (μ=1.003 cm^{-1}). The structure was solved by the direct method (SIR97) and refined by the full-matrix least-squares method on F^2 with anisotropic temperature factors for non-hydrogen atoms. All of the hydrogen atoms, except for the methine protons, were located at the calculated positions and refined with riding. The methine protons were located in the D map and refined with isotropic temperature factors. The final R1 and wR2 values are 0.092 (I>2σI) and 0.249 (all data) for 14911 reflections and 959 parameters.

Crystal data for ***1e[BF$_4$]***: Formula $C_{36}H_{27}F_4B$, M_w 546.41, black blocks, 0.40×0.25×0.20 mm^3, triclinic $P\bar{1}$, a=10.227(4) Å, b=10.201(3) Å, c= 14.472(3) Å, α=71.61(3)°, β=68.91(2)°, γ=85.82(3)°, V=1335.3(7) Å^3, ρ(Z=2)=1.359 g cm^{-3}. A total of 5657 unique data ($2\theta_{max}$=54.2°) were measured at T=123 K by a CCD apparatus ($Mo_{K\alpha}$ radiation, λ= 0.71070 Å). Numerical absorption correction was applied (μ= 0.963 cm^{-1}). The structure was solved by the direct method (SIR97) and refined by the full-matrix least-squares method on F^2 with anisotropic temperature factors for non-hydrogen atoms. All of the hydrogen atoms, except for the methine proton, were located at the calculated positions and refined with riding. The methine proton was located in the D map and refined with isotropic temperature factors. The final R1 and wR2 values are 0.068 (I>2σI) and 0.169 (all data) for 5657 reflections and 400 parameters.

Redox potential measurements: Redox potentials (E_{ox} and E_{red}) were measured by cyclic voltammetry in dry MeCN containing 0.1 mol dm^{-3} Et_4NClO_4 as a supporting electrolyte. Ferrocene undergoes one-electron oxidation at +0.38 V under the same conditions. All of the values shown in the text are shown in *E*/V versus SCE measured at the scan rate of 100 mV s^{-1}. A Pt disk and wire electrodes were used as the working and counterelectrodes, respectively. The working electrode was polished by using a water suspension of Al_2O_3 (0.05 μm) before use. The irreversible halfwave potentials were estimated from the anodic peak potentials (E^{pa}) as E^{ox}=E^{pa}−0.03 or the cathodic peak potentials (E^{pc}) as E^{red}=E^{pc}+0.03.

Computational method: The DFT calculations were performed with the Gaussian 98 program package.[27] The geometries of the compounds were optimized by the B3LYP method[28] in combination with a 6-31G* basis set without performing frequency calculations.

 © 2007 Wiley-VCH Verlag GmbH & Co. KGaA, Weinheim

Acknowledgements

This work was supported by a Grant-in-Aid for Scientific Research from the Ministry of Education, Science, and Culture (No. 17655012) and from JSPS (No. 18–4425). T.T. gratefully acknowledges a JSPS Research Fellowship for Young Scientist. We thank Prof. Tamotsu Inabe (Department of Chemistry, Faculty of Science, Hokkaido University) for the use of facilities to analyze the X-ray structures. Elemental analyses were performed at the Center for Instrumental Analysis of Hokkaido University. Mass spectra were measured by Mr. Kenji Watanabe and Dr. Eri Fukushi at the GC-MS&NMR Laboratory (Faculty of Agriculture, Hokkaido University).

[1] a) I. R. Epstein, W. N. Lipscomb, *Inorg. Chem.* **1971**, *10*, 1921–1928; b) W. N. Lipscomb, *Acc. Chem. Res.* **1973**, *6*, 257–262.

[2] A. J. Arduengo III, S. F. Gamper, M. Tamm, J. C. Calabrese, F. Davidson, H. A. Craig, *J. Am. Chem. Soc.* **1995**, *117*, 572–573.

[3] a) J. E. McMurry, T. Lectka, C. N. Hodge, *J. Am. Chem. Soc.* **1989**, *111*, 8867–8872; b) J. E. McMurry, T. Lectka, *J. Am. Chem. Soc.* **1990**, *112*, 869–870; c) J. E. McMurry, T. Lectka, *Acc. Chem. Res.* **1992**, *25*, 47–53; d) J. E. McMurry, T. Lectka, *J. Am. Chem. Soc.* **1993**, *115*, 10167–10173; e) R. P. Kirchen, T. S. Sorensen, *J. Am. Chem. Soc.* **1979**, *101*, 3240–3243; f) T. S. Sorensen, S. M. Whitworth, *J. Am. Chem. Soc.* **1990**, *112*, 8135–8144; g) C. Taeschler, T. S. Sorensen, *J. Mol. Model.* **2000**, *6*, 217–225; h) C. Taeschler, M. Parvez, T. S. Sorensen, *J. Phys. Org. Chem.* **2002**, *15*, 36–47.

[4] a) R. Ponec, G. Yuzhakov, D. J. Tantillo, *J. Org. Chem.* **2004**, *69*, 2992–2996; b) D. J. Tantillo, R. Hoffmann, *J. Am. Chem. Soc.* **2003**, *125*, 4042–4043.

[5] Very large value of pK_R^+ of 11.0 for 9-phenylacridinium indicates the stability of this cationic unit, see: J. W. Bunting, W. G. Meathrel, *Can. J. Chem.* **1973**, *51*, 1965–1972.

[6] a) W. B. Schweizer, G. Procter, M. Kaftory, J. D. Dunitz, *Helv. Chim. Acta*, **1978**, *61*, 2783–2808; b) V. Balasubramaniyan, *Chem. Rev.* **1966**, *66*, 567–641; c) H. E. Katz, *J. Am. Chem. Soc.* **1985**, *107*, 1420–1421; d) H. E. Katz, *J. Org. Chem.* **1985**, *50*, 5027–5032; e) H. A. Staab, T. Saupe, *Angew. Chem.* **1988**, *100*, 895–909; *Angew. Chem. Int. Ed. Engl.* **1988**, *27*, 865–879; f) P. C. Bell, J. D. Wallis, *Chem. Commun.* **1999**, 257–258.

[7] The pK_R^+ values of triphenylmethylium and dianisylphenylmethylium are −6.63 and −1.24, respectively, see: N. C. Deno, J. J. Jaruzelski, A. Schriesheim, *J. Am. Chem. Soc.* **1955**, *77*, 3044–3051.

[8] Generation, structure, and some properties of **1a**,**b**$^+$ were published as a preliminary communication. See ref. [9a].

[9] a) H. Kawai, T. Takeda, K. Fujiwara, T. Suzuki, *J. Am. Chem. Soc.* **2005**, *127*, 12172–12173; b) H. Kawai, T. Nagasu, T. Takeda, K. Fujiwara, T. Tsuji, M. Ohkita, J. Nishida, T. Suzuki, *Tetrahedron Lett.* **2004**, *45*, 4553–4558.

[10] a) R. Panisch, M. Bolte, T. Müller, *J. Am. Chem. Soc.* **2006**, *128*, 9676–9682; b) S. A. Reiter, S. D. Nogai, K. Karaghiosoff, H. Schmidbaur, *J. Am. Chem. Soc.* **2004**, *126*, 15833–15843.

[11] Previous studies on the "unsymmetric" triarylmethane-triarylmethylium complexes of $[Ar_3C\cdots H\cdots CAr'_3]^+$ ($Ar \neq Ar'$) revealed that they adopt form **A** geometry, yet the preference for the C–H-localized structure may be directly related to the inequivalency of the pK_R^+ of units of Ar_2C^+ and Ar'_2C^+, see ref. [9b].

[12] H. Wang, F. P. Gabbaï, *Angew. Chem.* **2004**, *116*, 186–189; *Angew. Chem. Int. Ed.* **2004**, *43*, 184–187.

[13] G. A. Olah, J. Lukas, *J. Am. Chem. Soc.* **1967**, *89*, 2227–2228.

[14] T. Suzuki, T. Nagasu, H. Kawai, K. Fujiwara, T. Tsuji, *Tetrahedron Lett.* **2003**, *44*, 6095–6098.

[15] H. Kawai, T. Takeda, K. Fujiwara, M. Wakeshima, Y. Hinatsu, T. Suzuki, unpublished results.

[16] K. Komatsu, H. Akamatsu, S. Aonuma, Y. Jinbu, N. Maekawa, K. Takeuchi, *Tetrahedron* **1991**, *47*, 6951–6966.

[17] a) H. H. Hodgson, J. S. Whitehurst, *J. Chem. Soc.* **1948**, 80–81; b) D. Seyferth, S. C. Vick, *J. Organomet. Chem.* **1977**, *141*, 173–187; c) Š. Vyskočil, L. Meca, I. Tišlerová, I. Císřová, M. Polášek, S. R. Harutyunyan, Y. N. Belokon, R. M. J. Stead, L. Farrugia, S. C. Lockhart, W. L. Mitchell, P. Kočovský, *Chem. Eur. J.* **2002**, *8*, 4633–4648.

[18] a) C. Wolf, X. Mei, *J. Am. Chem. Soc.* **2003**, *125*, 10651–10658; b) X. Mei, C. Wolf, *Chem. Commun.* **2004**, 2078–2079; c) X. Mei, C. Wolf, *J. Am. Chem. Soc.* **2004**, *126*, 14736–14737; d) X. Mei, R. M. Martin, C. Wolf, *J. Org. Chem.* **2006**, *71*, 2854–2861.

[19] a) N. Tanaka, T. Kasai, *Bull. Chem. Soc. Jpn.* **1981**, *54*, 3020–3025; b) W. D. Neudorff, D. Lentz, M. Anibarro, A. D. Schlüter, *Chem. Eur. J.* **2003**, *9*, 2745–2757.

[20] R. H. Mitchell, M. Chaudhary, R. V. Williams, R. Fyles, J. Gibson, M. J. Ashwood-Smith, A. J. Fry, *Can. J. Chem.* **1992**, *70*, 1015–1021.

[21] W. E. Bachmann, E. J. Chu, *J. Am. Chem. Soc.* **1936**, *58*, 1118–1121.

[22] E. Beschke, O. Beitler, S. Strum, *Liebigs Ann. Chem.* **1909**, *369*, 184–208.

[23] G. Wittig, H. Petri, *Chem. Ber.* **1935**, *68*, 924–927.

[24] D. B. DuPré, *J. Phys. Chem. A* **2005**, *109*, 622–628.

[25] L. J. Altman, P. Laungani, G. Gunnarson, H. Wennerström, S. Forsén, *J. Am. Chem. Soc.* **1978**, *100*, 8264–8266.

[26] a) T. Suzuki, T. Takeda, H. Kawai, K. Fujiwara, *In Strained Hydrocarbon: Ultralong C–C Bond*, Wiley-VCH, H. Dodziuk, Ed. **2007**; b) R. L. Clough, W. J. Kung, R. E. Marsh, J. D. Roberts, *J. Org. Chem.* **1976**, *41*, 3603.

[27] Gaussian 98: M. J. Frisch, G. W. Trucks, H. B. Schlegel, G. E. Scuseria, M. A. Robb, J. R. Cheeseman, V. G. Zakrzewski, J. A. Montgomery, Jr., R. E. Stratmann, J. C. Burant, S. Dapprich, J. M. Millam, A. D. Daniels, K. N. Kudin, M. C. Strain, O. Farkas, J. Tomasi, V. Barone, M. Cossi, R. Cammi, B. Mennucci, C. Pomelli, C. Adamo, S. Clifford, J. Ochterski, G. A. Petersson, P. Y. Ayala, Q. Cui, K. Morokuma, D. K. Malick, A. D. Rabuck, K. Raghavachari, J. B. Foresman, J. Cioslowski, J. V. Ortiz, B. B. Stefanov, G. Liu, A. Liashenko, P. Piskorz, I. Komaromi, R. Gomperts, R. L. Martin, D. J. Fox, T. Keith, M. A. Al-Laham, C. Y. Peng, A. Nanayakkara, C. Gonzalez, M. Challacombe, P. M. Gill, B. Johnson, W. Chen, M. W. Wong, J. L. Andres, C. Gonzalez, M. Head-Gordon, E. S. Replogle, J. A. Pople, Gaussian, Pittsburg, PA, **1998**.

[28] a) A. D. Becke, *J. Chem. Phys.* **1993**, *98*, 5648–5652; b) C. Lee, W. Yang, R. G. Parr, *Phys. Rev. B.* **1988**, *37*, 785–789; c) B. Miehlich, A. Savin, H. Stoll, H. Preuss, *Chem. Phys. Lett.* **1989**, *157*, 200.

Received: May 26, 2007
Published online: August 27, 2007

 © 2007 Wiley-VCH Verlag GmbH & Co. KGaA, Weinheim